SIMULTANEOUS DETERMINATION OF THE STRAIN HARDENING EXPONENT, THE SHEAR MODULUS AND THE YIELD STRESS IN AN INVERSE PROBLEM

SALİH TATAR, RAMAZAN TINAZTEPE, AND ZAHİR MURADOGLU

ABSTRACT. This paper is devoted to simultaneous determination of the strain hardening exponent, the shear modulus and the yield stress in an inverse problem. The inverse problem consists of determining the unknown coefficient $f = f(T^2), T^2 := |\nabla u|^2$ in the nonlinear equation $u_t - \nabla.\Big(f(T^2)\nabla u\Big) = 2t,\ (x, y, t) \in \ \Omega_{\mathcal{T}} := \Omega \times (0, \mathcal{T})$, $\Omega \subset \mathbb{R}^2$, by measured output data (or additional data) given in the integral form. After we solve direct problem using a semi-implicit finite difference scheme, a numerical method based on discretization of the minimization problem, steepest descent method and least squares method is proposed for the solution of the inverse problem. We use Tikhonov regularization to overcome the ill-posedness of the inverse problem. Numerical examples with noise free and noisy data illustrate applicability and accuracy of the proposed method to some extent.

Nomenclature

g: Modulus of plasticity
G: Modulus of rigidity (shear modulus)
E: Young's modulus
ν: Poisson coefficient
$\mathbb{F}$: Class of admissible coefficients
Ω: Cross section of a bar
$\partial\Omega$: Boundary of Ω
φ: Angle of twist per unit length
$T^2 := |\nabla u|^2$: Stress intensity
$u(x, y)$: Prandtl stress function
${T_0}^2 := \max_{x\in\Omega} |\nabla u|^2$: Yield stress
M: Theoretical value of the torque
$\mathcal{M}$: Measured value of the torque
$\mathcal{T}$: Final time
$< ., . >$: Inner product
$\|.\|_\infty$: Maximum norm
$\|.\|_2$: L_2 norm in Ω
$L_2(\Omega)$: Set of square integrable functions on Ω
$J(f)$: Cost functional
τ: Time step
w_h: Uniform mesh
h_1: Mesh step in x direction

Date: August 31, 2015.

Key words and phrases. Inverse problem; Minimization problem; Quasi-solution; Existence and uniqueness; Steepest descent method; Least squares approach.

h_2: Mesh step in y direction
N_1: Number of mesh points in x direction
N_2: Number of mesh points in y direction
N: Number of measurements
u: Exact solution
u_h: Approximate solution
u_0: Initial approximation
εu_h: Absolute error
$O(.)$: Landau's symbol
δu_h: Relative error
κ: Strain hardening exponent
$\mathbf{T}$: Transpose of a matrix
∇: Gradient
λ: Regularization parameter
ϵ: Stopping criterion
q: Number of points in t direction
h: Differential step for κ
k: Differential step for G
m: Differential step for ${T_0}^2$

1. Introduction

According to the deformation theory of plasticity, stress-strain relation between deviators is described by the Hencky correlation

$$\sigma_{ij}^D = 2g(\Gamma^2)\epsilon_{ij}^D, \quad i,j = 1,2,3.$$

Then the following relation holds between the intensities of shift strain $\Gamma := \left(2\epsilon_{ij}^D \epsilon_{ij}^D\right)^{\frac{1}{2}}$ and tangential stress $T := \left(\frac{1}{2}\sigma_{ij}^D \sigma_{ij}^D\right)^{\frac{1}{2}}$

$$T = g\left(\Gamma^2\right)\Gamma, \tag{1.1}$$

where the function $g\left(\Gamma^2\right)$ describes the elastoplastic properties of the material and is sometimes called the modulus of plasticity. Equation (1.1) can be formally regarded as a general condition encompassing different phases strain. Thus, putting $g\left(\Gamma^2\right) = \frac{\tau_s}{\Gamma}$, we obtain the Von Mises's criterion $T = \tau_s$; while putting $g\left(\Gamma^2\right) = G$, we obtain the case of Hooke's elastic medium, where $T = G\Gamma$ and $G = E/(2(1+\nu))$ is the modulus of rigidity (shear modulus), $E > 0$ is the Young's modulus, $\nu \in \left(0, \frac{1}{2}\right)$ is the Poisson coefficient. The shear modulus is defined as the ratio of shear stress to the shear strain. It describes an object's tendency to shear when acted upon by opposing forces. Also it is used to determine how elastic or bendable materials evolve if they are sheared, which is being pushed parallel from opposite sides. The Poisson coefficient for some materials such as aluminum, bronze, copper, ice, magnesium, molybdenum, monel metal, nickel silver are 0.334, 0.34, 0355, 0.33, 0.35, 0.307, 0.315, 0.322 respectively. Since the Poisson coefficient of the aforementioned materials are around 0.3, it is assumed to be 0.3 throughout this paper. We note that changing of this value affect numerical results but doesnt affect the applicability

and efficiency of the method given in Section 3.

According to the deformation theory of plasticity, the function $g\left(\Gamma^2\right)$ satisfies the following conditions [12]:

$$\begin{cases} c_1 \leq g(\Gamma^2) \leq c_2, \\ g(\Gamma^2) + 2g'(\Gamma^2)\Gamma^2 \geq c_3 > 0, \forall \Gamma^2 \in \left[{\Gamma_*}^2, \Gamma^{*2}\right], \\ g'(\Gamma^2) \leq 0, \\ \exists {\Gamma_0}^2 \in ({\Gamma_*}^2, \Gamma^{*2}) : \ g(\Gamma^2) = G, \ \forall \Gamma^2 \in \left[{\Gamma_0}^2, \Gamma^{*2}\right], \end{cases} \tag{1.2}$$

where $c_i > 0, \ i = 1, 2, 3$ are constants. Thus $g(\Gamma^2)$ is a decreasing function of Γ^2 with $c_1 \leq g(\Gamma^2) \leq c_2$, there exists an inverse function $\Gamma = f(T^2)T$ such that $g(\Gamma^2)f(T^2) = 1$ and $f(T^2)$ satisfies the following conditions [12]:

$$\begin{cases} c_4 \leq f(T^2) \leq c_5, \\ c_4 \leq f(T^2) + 2f'(T^2)T^2 \leq c_6, \forall T^2 \in \left[{T_*}^2, T^{*2}\right], \\ f'(T^2) \geq 0, \\ \exists {T_0}^2 \in ({T_*}^2, T^{*2}) : \ f(T^2) = \dfrac{1}{G}, \ \forall T^2 \in \left[{T_0}^2, T^{*2}\right], \end{cases} \tag{1.3}$$

where $c_4 = \dfrac{1}{c_2}$, $c_5 = \dfrac{1}{c_1}$ and $c_6 = \dfrac{1}{c_3}$. A set $\mathbb{F}$ satisfying the conditions (1.3) is called the class of admissible coefficients in optimal control and inverse problems theory.

The quasistatic mathematical model of the elastoplastic torsion of a strain hardening bar is given in [11]. In this model, one seeks the solution $u(x, y), (x, y) \in \Omega \subset \mathbb{R}^2$, of the following nonlinear boundary value problem:

$$\begin{cases} -\nabla.\big(f(T^2)\nabla u\big) = 2\varphi, \ (x, y) \in \Omega \subset \mathbb{R}^2, \\ u(x, y) = 0, \quad (x, y) \in \partial\Omega, \end{cases} \tag{1.4}$$

where $\Omega := (0, a) \times (0, b)$, $a, b > 0$ is the cross section of a bar, φ is the angle of twist per unit length, $T^2 := |\nabla u|^2$ is the stress intensity and $u(x, y)$ is the Prandtl stress function. Now we define the parameters in (1.3). First, we define ${T_0}^2 := \max\limits_{x \in \Omega} |\nabla u|^2$. In materials science, it corresponds to the yield stress which is the maximum stress or force per unit area within a material that can arise before the onset of permanent deformation. When stresses up to the yield stress are removed, the material resumes its original size and shape. In other words, there is a temporary shape change that is self-reversing after the force is removed, so that the object returns to its original shape. This kind of deformation is called pure elastic deformation. On the other hand,

irreversible deformations are permanent even after stresses have been removed. One type of irreversible deformation is pure plastic deformation. For such materials the yield stress marks the end of the elastic behavior and the beginning of the plastic behavior. For any angle $\varphi > 0$, all points of the bar have non-zero stress intensity which means the condition ${T_*}^2 > 0$ in (1.3) makes sense. It is also known that in order for the equation in (1.4) to be elliptic, the first two conditions in (1.3) are necessary. Further, the last condition of (1.3) means that the elastic deformations precede the plastic ones.

Let $u = u(x, y, \varphi; f)$ be the solution of the nonlinear boundary value problem (1.4) for an angle φ and a function f. Then theoretical value of the torque (moment of force) is given by

$$M[f](\varphi) = 2 \int_{\Omega} u(x, y, \varphi; f) dx\, dy,\ \varphi \in [\varphi_*, \varphi^*],\ \varphi_* > 0, \tag{1.5}$$

i.e., the torque is equal to twice the volume enclosed within the stress surface $u(x, y)$ [11].

For a given function $f(T^2)$ and the angle φ, the problem (1.4) is called the direct (forward) problem. The associated inverse problem consists of determining the pair of functions $\left\{u(x, y), f(T^2)\right\}$ from the following nonlocal nonlinear identification problem:

$$\begin{cases} -\nabla.\big(f(T^2)\nabla u\big) = 2\varphi,\ (x, y) \in \Omega \subset \mathbb{R}^2, \\ u(x, y) = 0, \quad (x, y) \in \partial\Omega, \\ 2 \int\limits_{\Omega} u(x, y; \varphi_i) dx\, dy = \mathcal{M}_i,\ i = 1, \cdots, N, \end{cases} \tag{1.6}$$

where $\mathcal{M}_i := \mathcal{M}(\varphi_i)$ are the measured values of the torque, (measured output data) corresponding to the angles φ_i, $i = 1, \cdots, N$ and $N > 1$ is the number of measurements. These discrete values are assumed to be given during the quasistatic process of torsion, given by the angle of twist $\varphi_i \in [\varphi_*, \varphi^*]$. Therefore in the considered physical model the quasistatic process of torsion is simulated by the monotone increasing values $0 < \varphi_* = \varphi_1 < \varphi_2 < \cdots < \varphi_N = \varphi^*$ of the angle $\varphi \in [\varphi_*, \varphi^*]$. Hence the torque, defined by (1.5), may be considered as a function of the angle $\varphi > 0$. The direct problem (1.4) and the inverse problem (1.6) have been well-studied both theoretically and numerically in the mathematical literature (see [6], [7], [8], [22], [23], [24]).

However in real applications the torsion process is not quasistatic, it depends on the time. The mathematical model of the real torsion process is given by the following evolutional problem:

$$\begin{cases} u_t - \nabla.\big(f(T^2)\nabla u\big) = 2t, \ (x,y,t) \in \Omega_{\mathcal{T}}, \\ u(x,y,0) = 0, \quad (x,y) \in \Omega, \\ u(x,y,t) = 0, \quad (x,y,t) \in \partial\Omega \times (0,\mathcal{T}), \end{cases} \tag{1.7}$$

where $\Omega_{\mathcal{T}} := \Omega \times (0,\mathcal{T})$ and $\mathcal{T}$ is a final time. The associated inverse problem consists of determining the pair of functions $\Big\{u(x,y,t), f(T^2)\Big\}$ from the following nonlocal nonlinear identification problem:

$$\begin{cases} u_t - \nabla.\big(f(T^2)\nabla u\big) = 2t, \ (x,y,t) \in \Omega_{\mathcal{T}}, \\ u(x,y,0) = 0, \quad (x,y) \in \Omega, \\ u(x,y,t) = 0, \quad (x,y,t) \in \partial\Omega \times (0,\mathcal{T}), \\ 2\displaystyle\int_{\Omega} u(x,y;t_i)dx\,dy = \mathcal{M}(t_i), \ i = 1, \cdots, N, \end{cases} \tag{1.8}$$

where $\mathcal{M}_i := \mathcal{M}(t_i), \ i = 1, \cdots, N$ are the measured values of the torque. Similar to (1.5), the theoretical value of the torque is defined by

$$M[f](t) = 2\int_{\Omega} u(x,y,t;f)dx\,dy, \ t \in [t_*, t^*], \ t_* > 0, \tag{1.9}$$

where $u(x,y,t;f)$ is a solution of (1.7) for a given function f.

The direct problem (1.7) and the inverse problem (1.8) have been well-studied both theoretically and numerically in the mathematical literature [25].

Now we define the quasi-solution of the inverse problem (1.8). For this purpose, we reformulate the inverse problem. We denote the unique solution of the nonlinear direct problem (1.7) by $u(x,y,t;f)$ for a given $f \in \mathbb{F}$. Then for each $t \in (0,\mathcal{T})$, the inverse coefficient problem can be formulated as the following nonlinear functional equation:

$$2\int_{\Omega} u(x,y,t;f)dx\,dy = M(t), \quad f \in \mathbb{F}. \tag{1.10}$$

Let $\mathring{H}^1(\Omega) := \Big\{v \in H^1(\Omega) : v = 0 \, on \, \partial\Omega\Big\}$ and $V = L^2\left(0,\mathcal{T};\mathring{H}^1(\Omega)\right)$. Then the weak solution of the direct problem (1.7) is defined as a solution of the following abstract operator equation:

$$Lu + Au = F, \tag{1.11}$$

where the nonlinear operator $A : V \to V^\star$ and the linear functional F are defined by

$$< Au, v >_V = \int_0^{\mathcal{T}} \int_\Omega f(|\nabla u|^2)\nabla u \nabla v \, dx \, dy \, dt, \forall u, v \in V,$$

$$< F, v >_V = \int_0^{\mathcal{T}} \int_\Omega s(x, y, t)v(x, y, t) \, dx \, dy \, dt, \forall v \in V,$$

$s(x, y, t) = 2t$ and $L := D(L) \subset V \to V^\star$ is defined by $Lu = u_t$. We obtain the weak solution of the problem (6) by multiplying the evolution equation by a function $v \in V$, and then integrating the resulting equation using integration by parts. Based on this weak solution, we can define the following cost functional

$$J(f) = \int_0^{\mathcal{T}} \left[2 \int_\Omega u(x, y, t; f) dx \, dy - \mathcal{M}(t) \right]^2 dt, \ f \in \mathbb{F}. \tag{1.12}$$

A quasi-solution of the inverse problem (1.8) is defined as a solution of the following minimization problem:

$$J(f_*) = \inf_{f \in \mathbb{F}} J(f). \tag{1.13}$$

In [25], continuity of the functional $J(f)$ and compactness of the class of admissible coefficients $\mathbb{F}$ are proved. This means the inverse problem (1.8) has a quasi-solution.

In the last years, there are some works related to simultaneously determination of unknowns in an inverse problem, for example, see [13], [26]. To the best of the authors knowledge, there is no work related to determination of the strain hardening exponent κ, the shear modulus G and the yield stress ${T_0}^2$ simultaneously in an inverse problem, while there are many papers that investigate the determination of the material properties, for example, see [1], [2], [9], [10], [14], [15], [16], [19], [21], [27]. This paper achieves that to some extent.

This article is organized as follows: In the next section, we solve the nonlinear direct problem (1.7) and analyze the numerical solution. In Section 3, we present our method. Some numerical examples are given to show the efficiency of the method in Section 4 . The conclusions, possible directions and applications to the engineering problems are given in Section 5.

2. Numerical solution of the nonlinear direct problem

In this section, we solve the nonlinear direct problem (1.7). For the numerical solution, the following semi-implicit finite difference scheme is used:

$$\frac{v_{i,j}^{(k+1)}-v_{i,j}^{(k)}}{\tau}-\frac{1}{h_1}\left[\tilde{f}_{i+1/2,j}\frac{v_{i+1,j}^{(k+1)}-v_{i,j}^{(k+1)}}{h_1}-\tilde{f}_{i-1/2,j}\frac{v_{i,j}^{(k+1)}-v_{i-1,j}^{(k+1)}}{h_1}\right]$$
$$-\frac{1}{h_2}\left[\tilde{f}_{i,j+1/2}\frac{v_{i,j+1}^{(k+1)}-v_{i,j}^{(k+1)}}{h_2}-\tilde{f}_{i,j-1/2}\frac{v_{i,j}^{(k+1)}-v_{i,j-1}^{(k+1)}}{h_2}\right]=2t^{(k+1)},$$

where $(x_i,y_j)\in w_h$, $w_h:=\left\{(x_i,y_j):\ x_i=ih_1,\ y_j=jh_2,\ i=\overline{0,N_1-1},\ j=\overline{0,N_2-1}\right\}$ is the piecewise uniform mesh with the mesh steps $h_1=a/(N_1-1)$, $h_2=b/(N_2-1)$, $v_{i,j}:=u^{(k)}(x_i,y_j)$ are the nodal values of the function (kth iteration), and τ is the time step. The coefficients $\tilde{f}_{p,q}$ are defined as follows:

$$\tilde{f}_{i\pm1/2,j}=f\left(\left|\nabla u^{(k)}(x_{i\pm1/2},y_j)\right|^2\right),\ \tilde{f}_{i,j\pm1/2}=f\left(\left|\nabla u^{(k)}(x_i,y_{j\pm1/2})\right|^2\right).$$

The accuracy of the above difference scheme is $O(h_1^2+h_2^2+\tau)$. It is well known that the above semi-implicit finite difference scheme is unconditionally stable and does not suffer from any time step size restriction. In other words, while explicit schemes for very small time steps which leads to poor efficiency and limits their practical use, the semi-implicit scheme is stable for all time steps.

We note that solution of the inverse problem is closely related to solution of the direct problem since the outputs of the numerical solution of the direct problem are used as inputs for the inverse problem. Therefore, we test the difference scheme on some numerical examples. The first series of the numerical experiments is related to numerical solution of the nonlinear direct problem (1.7). For this purpose, $u(x,y,t)=sin(\pi x)\,sin(\pi y)\,t$ is taken to be analytical solution of the nonlinear equation $u_t-\nabla.\left(g(|\nabla u|^2)\nabla u\right)=F(x,y,t)$ with the function $f(T^2)=\dfrac{1}{\sqrt{1+T^2}}$, $T^2=u_x^2+u_y^2$ and appropriately chosen source function $F(x,y,t)$. It is clear that $u(x,y,t)$ satisfies both initial and

boundary conditions in (1.7). In solving the nonlinear direct problem, iterations are repeated until convergence is reached in the sense that

$$\max_{(x_i,y_j)\in w_h} \left| u_{i,j}^{(n)} - u_{i,j}^{(n-1)} \right| < \varepsilon,$$

where $\varepsilon > 0$ is a given stopping criterion. We take $a = b = 1$ and $t \in (0, 1)$. The other inputs are shown in Table 1 for $t = 0.5$. The absolute error, defined by $\varepsilon u_h = \left\|(u - u_h)\right\|_\infty$ and the relative error, defined by $\delta u_h = \left\|(u - u_h)/u\right\|_\infty$ are also shown in Table 1, where $\left\|.\right\|_\infty$ denotes maximum norm, u and u_h denote the exact and approximate solutions of the nonlinear direct problem respectively. As it is seen in the Table 1, we test the above difference scheme for some different number of the mesh points N_1 and N_2, the time step τ, the stopping criterion ε and the initial approximation u_0. The experiments clearly indicate that the initial guess is the main factor affecting the accuracy of the solutions. As the first initial approximation, the function $u_0 \equiv 0$ is taken which satisfies both initial and boundary conditions in (1.7). The number of the iterations are found to be around 10 at each time t. This is closely related with the choice of the initial approximation u_0. The function $u_0 = t\,(x^2 - x)\,(y^2 - y)$ is taken another initial approximation which also satisfies both initial and boundary conditions in (1.7). In this case, the corresponding absolute and relative errors are relatively increased. The effect of the initial approximation becomes apparent in the last two experiments where $u_0 = x^2 + yt + 1$ is taken to be an initial approximation which satisfies neither the initial condition nor the boundary condition, and it is observed that the results are not satisfactory. The number of iterations are found to be around 70 for the last initial approximation. One way to overcome this difficulty is to choose the initial approximation closely enough to both initial and boundary conditions. It should also be noted that the same initial guesses for different mesh points are applied and it is observed that they are not very far from the exact solution. In the seventh experiment, the time step τ is taken to be 0.001, but the corresponding absolute and relative errors are increased because of the computational noise factors. Based on above results, the sixth experiment is optimal and quite satisfactory. So the parameters $N_1 = N_2 = 41$, $\tau = 0.01$ and $\varepsilon = 10^{-5}$ are taken optimal ones in all computational experiments below. It also seems that the initial iteration $u_0 = 0$ is optimal for the numerical solution of the nonlinear direct problem (1.7) since it satisfies both initial and boundary conditions.

Next we examine the above difference scheme by using its convergence order. The convergence order is found by the following useful formula: [6], [20]

$$\text{Convergence order:}=\log_{\frac{h_1}{h_2}} \frac{\varepsilon u_{h_1}}{\varepsilon u_{h_2}}.$$

By Table 1, for $N_1 = N_2 = 20$, $N_1 = N_2 = 40$, $\tau = 0.1$ and $\varepsilon = 10^{-4}$, the convergence order of space is found to be 2.03 as expected with the order $O(h_1^2 + h_2^2 + \tau)$ of the method. For $\tau_1 = 0.1$, $\tau_2 = 0.2$, $N_1 = N_2 = 40$ and $\varepsilon = 10^{-4}$ the convergence order of time is found to be 1.04 as expected with the order $O(h_1^2 + h_2^2 + \tau)$ of the method.

For many engineering materials, the function $f(T^2)$ in (1.4) has the following form:

$$f(T^2) = \begin{cases} 1/G, & T^2 \le {T_0}^2, \\ 1/G \ \left(T^2/{T_0}^2\right)^{0.5(1-\kappa)}, & {T_0}^2 < T^2, \end{cases} \tag{2.1}$$

which corresponds to the Ramberg-Osgood curve $\sigma_i = \sigma_0(e_i/e_0)^\kappa$, where $\kappa \in (0, 1)$ is the strain hardening exponent. The values $\kappa = 1$ and $\kappa = 0$ correspond to pure elastic and pure plastic cases respectively. Evidently, this function satisfies all conditions in (1.3). The Young's modulus E are taken as $E = 210$ Gpa (equivalently $G = 80.77$ Gpa) and $E = 110$ Gpa (equivalently $G = 42.30$ Gpa); the yield stress ${T_0}^2$ are taken as ${T_0}^2 = 0.027$ and ${T_0}^2 = 0.020$ for stiff and soft engineering materials respectively, [6], [7], [8], [22], [23]. The nonlinear direct problem (1.7) is solved for the function $f(T^2)$, defined by (2.1), and the torques for a few times are obtained by applying the numerical integration trapezoidal formula. The results are shown in Table 2 and Table 3. These and more such pairs $(t_i, \mathcal{M}_i)$ will be used as input data for the numerical solution of the inverse problem. We also compute the value of $\max\limits_{x\in\Omega} |\nabla u|^2$ for each time and find that this value is less than 0.027 and 0.020 respectively for the first experiments ($i = 1$) in Table 2 and Table 3, which means $i = 1$ corresponds to the elastic case. But the other experiments correspond to the plastic cases as shown in Table 2 and Table 3.

In the pure elastic case, the nonlinear direct problem (1.7) becomes

$$\begin{cases} u_t - k\Delta u = 2t, & (x, y, t) \in \Omega_{\mathcal{T}}, \\ u(x, y, 0) = 0, & (x, y) \in \Omega, \\ u(x, y, t) = 0, & (x, y, t) \in \partial\Omega \times (0, \mathcal{T}), \end{cases} \tag{2.2}$$

where $k = 1/G$. The solution of the problem (2.2) is given by [18]

$$u(x,y,t) = \int_0^t \sum_{n=1}^{\infty} B_{mn}(s) \sin\left(\frac{m\pi x}{a}\right) \sin\left(\frac{n\pi y}{b}\right) e^{\left(-k\pi^2\left(\frac{m^2}{a^2}+\frac{n^2}{b^2}\right)\right)\left(t-s\right)} ds,$$

where $B_{mn} = \dfrac{4}{ab} 2s \displaystyle\int_\Omega \sin\left(\frac{m\pi x}{a}\right) \sin\left(\frac{n\pi y}{b}\right) dx\, dy;\ m,n \in \mathbb{N}\times\mathbb{N}$. It is clear from (2.2) that although the problem (1.7) is nonlinear, it is reduced to a linear one in the pure elastic case. Some applications of this formula can be found in [25]. We also verify our numerical results in Table 2 and Table 3 for pure elastic case ($i = 1$) by using the above explicit formula. The absolute error and the relative error is found around 10^{-4} and 15% respectively, which are in acceptable bounds since the values of torque is very small in the pure elastic cases.

As it is known, a problem is said to be well-posed or properly-posed in the sense of Hadamard if it has the following three properties: There exists a solution of the problem (existence), there is at most one solution of the problem (uniqueness), the solution depends continuously on the data (stability). If at least one of these properties does not hold then the problem is called ill-posed or improperly-posed. As it is known in the inverse problems field, like most inverse problems of the mathematical physics, the inverse coefficient problems for parabolic equations are severely ill-posed problems since the third condition is not satisfied, that is, small changes in the input data may lead to large deviations in the output. To show this feature of the inverse problem (1.8), two values $\kappa_1 = 0.2$ and $\kappa_2 = 0.8$ of the strain hardening exponent are taken and the corresponding functions $f(T^2)$ are drawn in Figure 1 (right figures) for stiff and soft materials respectively. Also the torques are found from numerical solution of the corresponding direct problems and numerical integration trapezoidal formula (left figures). This Figure shows that, for each class of the materials, the outputs are close enough although the functions $f(T^2)$ are quite different. This result illustrates the ill-posedness of the considered inverse problem.

TABLE 1. Data for two initial iterations and corresponding errors.

No	N_1	N_2	τ	ε	u_0	εu_h	δu_h
1	11	11	0.1	10^{-4}	0	4.8×10^{-3}	1.8×10^{-2}
2	21	21	0.1	10^{-4}	0	1.1×10^{-3}	5.7×10^{-3}
3	41	41	0.1	10^{-4}	0	2.7×10^{-4}	1.5×10^{-3}
4	41	41	0.05	10^{-4}	0	3.0×10^{-5}	3.4×10^{-4}
5	41	41	0.05	10^{-5}	0	2.9×10^{-5}	3.3×10^{-4}
6	41	41	0.01	10^{-5}	0	9.5×10^{-6}	1.9×10^{-4}
7	41	41	0.001	10^{-5}	0	2.9×10^{-4}	1.5×10^{-3}
8	41	41	0.05	10^{-5}	$t(x^2 - x)(y^2 - y)$	2.9×10^{-4}	1.5×10^{-3}
9	41	41	0.01	10^{-5}	$t(x^2 - x)(y^2 - y)$	2.9×10^{-4}	1.5×10^{-3}
10	41	41	0.05	10^{-5}	$x^2 + yt + 1$	5.7×10^{-1}	5.6
11	41	41	0.01	10^{-5}	$x^2 + yt + 1$	5.0×10^{-1}	4.0
12	21	21	0.001	10^{-7}	$x^2 + yt + 1$	4.8×10^{-1}	2.4
13	21	21	0.0001	10^{-9}	$x^2 + yt + 1$	4.8×10^{-1}	2.4

TABLE 2. Synthetic noise free data for stiff materials: $E = 210$ Gpa, ${T_0}^2 = 0.027$, $\kappa = 0.5$.

i	t_i	M_i	Elastic	Plastic
1	0.04	0.0037	$\surd$	
2	0.2	0.0708		$\surd$
3	0.4	0.2457		$\surd$
4	0.6	0.4897		$\surd$
5	0.8	0.7764		$\surd$

TABLE 3. Synthetic noise free data for soft materials: $E = 110$ Gpa, ${T_0}^2 = 0.020$, $\kappa = 0.7$.

i	t_i	M_i	Elastic	Plastic
1	0.04	0.036	$\surd$	
2	0.1	0.0191		$\surd$
3	0.3	0.1411		$\surd$
4	0.5	0.3440		$\surd$
5	0.7	0.6011		$\surd$

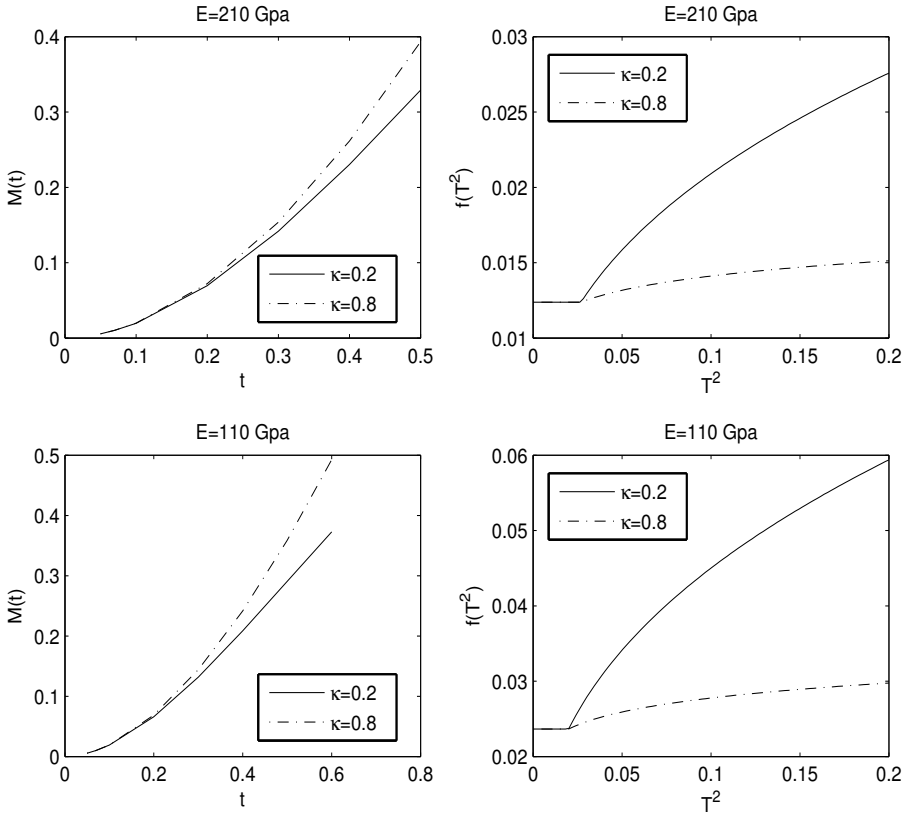

FIGURE 1. Illustration of the ill-posedness of the inverse problem

3. Overview of the method

In this section, first we explain and compare the two classical methods for finding the numerical solution of (1.6), i.e., the parametrization method and semi-analytic inversion method then we present our numerical method . The parametrization method is based on the discretization of the unknown curve (2.1), by using a piecewise linear continuous curve $f_h(T^2)$, which has the form [8]:

$$f_h(T^2)=\begin{cases} \beta_0=1/G,\ T^2\in\big(0,{T_0}^2\big], \\ \beta_0-\beta_1\big(T^2-{T_0}^2\big),\ T^2\in\big({T_0}^2,{T_1}^2\big], \\ \beta_0-\sum\limits_{i=1}^{N-1}\Big[\beta_i({T_i}^2-{T_{i-1}}^2)\Big]-\beta_N\big(T^2-T_{N-1}^2\big),\ T^2\in\big({T_{N-1}}^2,{T_N}^2\big]. \end{cases}$$

In the parametrization method, the unknown parameters $\beta_i>0,\ i=\overline{1,N}$ need to be determined step by step, beginning from the parameter

$\beta_0 = 1/G$. At each ith state, one needs to determine the parameter β_i using the pair $\big(\varphi_i, \mathcal{M}_i\big)$.

Although the parametrization algorithm is used for numerical solution of some class of inverse coefficients problems, it has some disadvantages. The first one is that the application of this method requires a huge amount of measured output data. This is of course undesirable since getting these data is costly. The second one is that the unknown curve can not be determined completely, but only partially. The third one is the ill-posedness of the method. This situation is illustrated in [8] and a regularization method is proposed.

To overcome these difficulties a new method, called the semi-analytic inversion method, is introduced in [7]. The semi-analytic inversion method is based on the determination of the three main unknowns of (2.1), namely the shear modulus $G > 0$, the yield stress ${T_0}^2$ and the strain hardening exponent $\kappa \in (0, 1)$. The first distinguishable feature of this algorithm is that it uses only a few values of the data $\big(\varphi_i, \mathcal{M}_i\big)$. Furthermore, the new method determines the unknown curve completely. The second distinguishable feature of this method is its well-posedness. Despite these favorable features, in the semi-analytic inversion method the algorithm used for determination of the yield stress is complicated and it needs many parameters to be determined before applying it. This is the main disadvantage of the semi-analytic inversion method. Because of this reason, a modification of the semi-analytic inversion method is given and analyzed in [24]. The modified semi-analytic inversion method does not require complicated calculations and it finds the yield stress using a minimum number of parameters.

In both parametrization and semi-analytic inversion method, the following error functional is minimized:

$$\max_{\varphi\in[\varphi_*,\varphi^*]} \left| 2\int_\Omega u(x,y;f;\varphi)dxdy - \mathcal{M}(\varphi) \right|, f \in \mathbb{F}.$$

Using the error functional above and modifying these two methods accordingly, one can apply them to the inverse problem (1.8), see [25] for details. But in the inverse problems of parabolic and hyperbolic type, the error functional in the form (1.12) is more useful and reasonable, [3], [4], [5], [17].

In our method we minimize the error functional given by $J(f)$ in (1.12). Since $f(T^2)$ is in the form of (2.1), the optimal $f(T^2)$ will be sought among the functions of the form (2.1). In this case, the

error functional is reduced to a real valued function of three variables, because f is defined via κ, G and ${T_0}^2$. We denote the function f corresponding to κ, G and ${T_0}^2$ as $f_{(\kappa,G,{T_0}^2)}$ and the solution of the direction problem corresponding to $f_{(\kappa,G,{T_0}^2)}$ $\big($i.e. $u(x,y,t;f_{(\kappa,G,{T_0}^2)})$ $\big)$ as $u_{(\kappa,G,{T_0}^2)}(x,y,t)$. Now the error functional defined by (1.12) can be written as

$$\begin{aligned} J(\kappa,G,{T_0}^2) &= \left\| 2\int_\Omega u_{(\kappa,G,{T_0}^2)}(x,y,t)dxdy - \mathcal{M}(t) \right\|_2^2 \\ &= \int_0^{\mathcal{T}} \left[2\int_\Omega u_{(\kappa,G,{T_0}^2)}(x,y,t)dxdy - \mathcal{M}(t) \right]^2 dt. \end{aligned}$$

Since the continuity of this functional is proved in the set of admissible functions $\mathbb{F}$, this functional now a function of three variables is continuous. The method for minimizing $J(\kappa,G,{T_0}^2)$ depends on the properties of J, e.g., convexity, differentiability and etc. In our case, the convexity or differentiability of $J(\kappa,G,{T_0}^2)$ is not clear due to the term $u_{\kappa,G,{T_0}^2}(x,y,t)$. However, we do not envision a major drawback in assuming the differentiability of $J(\kappa,G,{T_0}^2)$ in numerical implementations. For this reason, we proceed the minimization of $J(\kappa,G,{T_0}^2)$ by the steepest descent method which will utilize the gradient of J. In this method, the algorithm starts with an initial point $\big(\kappa_0,G_0,({T_0}^2)_0\big)$, then the point providing the minimum is approximated by the points

$$\big(\kappa_{i+1},G_{i+1},({T_0}^2)_{i+1}\big) = \big(\kappa_i,G_i,({T_0}^2)_i\big) + \big(\triangle\kappa_i,\triangle G_i,\triangle({T_0}^2)_i\big),$$

where $\big(\triangle\kappa_i,\triangle G_i,\triangle({T_0}^2)_i\big)$ is the feasible direction which minimizes the function

$$A_i(\triangle\kappa,\triangle G,\triangle T_0^2) = J\big((\kappa_i,G_i,({T_0}^2)_i) + (\triangle\kappa,\triangle G,\triangle T_0^2)\big).$$

This procedure is repeated until a stopping criterion is satisfied, i.e,

$$\left\| (\triangle\kappa_i,\triangle G_i,\triangle({T_0}^2)_i) \right\|_2 < \epsilon$$

or

$$\left| J(\kappa_{i+1},G_{i+1},({T_0}^2)_{i+1}) - J(\kappa_i,G_i,({T_0}^2)_i) \right| < \epsilon$$

or a certain number of iterations. In minimization of

$$J\big((\kappa_i,G_i,({T_0}^2)_i) + (\triangle\kappa,\triangle G,\triangle T_0^2)\big)$$

, we use the following estimate on $u_{(\kappa_i,G_i,({T_0}^2)_i))+(\triangle\kappa,\triangle G\triangle T_0^2)}(x,y,t)$:

$$u_{(\kappa_i,G_i,(T_0{}^2)_i)+(\triangle\kappa,\triangle G,\triangle T)}(x,y,t) \simeq u_{(\kappa_i,G_i,(T_0{}^2)_i)}(x,y,t) + \left\langle \nabla u_{(\kappa_i,G_i,(T_0{}^2)_i)}(x,y,t), (\triangle\kappa,\triangle G,\triangle T_0{}^2) \right\rangle,$$

where ∇ denotes the gradient of $u_{(\kappa,G,T_0{}^2)}(x,y,t)$ with respect to $(\kappa, G, T_0{}^2)$. Hence $A_i(\triangle\kappa,\triangle G,\triangle T_0{}^2)$ turns out to be the following:

$$A_i(\triangle\kappa,\triangle G,\triangle T_0{}^2) = \Bigg\| 2\int_\Omega \Bigg[u_{(\kappa_i,G_i,(T_0{}^2)_i)}(x,y,t) + \left\langle \nabla u_{(\kappa_i,G_i,(T_0{}^2)_i)}(x,y,t)\cdot(\triangle\kappa,\triangle G,\triangle T_0{}^2) \right\rangle \Bigg] dxdy - \mathcal{M}(t) \Bigg\|_2^2 + \lambda \left\| (\triangle\kappa,\triangle G,\triangle T_0{}^2) \right\|_2^2,$$

where λ denotes the regularization parameter which will be needed in handling the noisy data.

In numerical calculations, we note that $\|\cdot\|_2$ can be discretized by using a finite number of points in $[0,\mathcal{T}]$. We set $t_1 = 0 < t_2 < \cdots < t_q = \mathcal{T}$, hence $A_i(\triangle\kappa,\triangle G,\triangle T_0{}^2)$ has its new form as

(3.1)

$$A_i(\triangle\kappa,\triangle G,\triangle T_0{}^2) \simeq \sum_{k=1}^{q} \Bigg(2\int_\Omega u_{(\kappa_i,G_i,(T_0{}^2)_i))}(x,y,t_k)dxdy + 2\int_\Omega \left\langle \nabla u_{(\kappa_i,G_i,(T_0{}^2)_i))}(x,y,t_k), (\triangle\kappa,\triangle G,\triangle T_0{}^2) \right\rangle dxdy - \mathcal{M}(t_k) \Bigg)^2 + \lambda \left\| (\triangle\kappa,\triangle G,\triangle T_0{}^2) \right\|_2^2.$$

Now the minimization of this problem is a least squares problem whose solution leads to the following normal equation

$$(\lambda I + A^{\mathbf{T}}A)(\triangle\kappa,\triangle G,\triangle T_0{}^2)^{\mathbf{T}} = A^{\mathbf{T}}K,$$

where

$$A = \Bigg[\left(2\int_\Omega \nabla u_{(\kappa_i,G_i,(T_0{}^2)_i)}(x,y,t_1)dxdy \right)^{\mathbf{T}} \cdots \left(2\int_\Omega \nabla u_{(\kappa_i,G_i,(T_0{}^2)_i)}(x,y,t_q)dxdy \right)^{\mathbf{T}} \Bigg],$$

and

$$K = \Bigg[2\int_{\Omega} u_{(\kappa_i,G_i,(T_0{}^2)_i)}(x,y,t_1)dxdy - \mathcal{M}(t_1)\cdots \\ 2\int_{\Omega} u_{(\kappa_i,G_i,(T_0{}^2)_i)}(x,y,t_q)dxdy - \mathcal{M}(t_q)\Bigg]^{\mathbf{T}}.$$

Now the optimal direction is found by

$$(\triangle\kappa, \triangle G, \triangle T_0{}^2)^{\mathbf{T}} = (\lambda I + A^{\mathbf{T}}A)^{-1}A^{\mathbf{T}}K. \tag{3.2}$$

In forming A, the computation of the vector

$$\nabla u_{(\kappa_i,G_i,(T_0{}^2)_i)}(x,y,t_k) = \left(\nabla_{\kappa} u_{(\kappa_i,G_i,(T_0{}^2)_i)}(x,y,t_k), \nabla_{G} u_{(\kappa_i,G_i,(T_0{}^2)_i)}(x,y,t_k)\right)$$

can be achieved by the following estimates:

(3.3)
$$\nabla_{\kappa} u_{(\kappa_i,G_i,(T_0{}^2)_i)}(x,y,t_k) = \frac{u_{(\kappa_i+h,G_i,(T_0{}^2)_i)}(x,y,t_k) - u_{(\kappa_i,G_i,(T_0{}^2)_i)}(x,y,t_k)}{h},$$

(3.4)
$$\nabla_{G} u_{(\kappa_i,G_i,(T_0{}^2)_i)}(x,y,t_k) = \frac{u_{(\kappa_i,G_i+k,(T_0{}^2)_i)}(x,y,t_k) - u_{(\kappa_i,G_i,(T_0{}^2)_i)}(x,y,t_k)}{k},$$

(3.5)
$$\nabla_{T_0{}^2} u_{(\kappa_i,G_i,(T_0{}^2)_i)}(x,y,t_k) = \frac{u_{(\kappa_i,G_i,(T_0{}^2)_{i+m})}(x,y,t_k) - u_{(\kappa_i,G_i,(T_0{}^2)_i)}(x,y,t_k)}{m},$$

where h, k and m are the differential steps for κ,G and $T_0{}^2$.

The algorithm can be summarized as the following steps:

Step1. Set $(\kappa_0, G_0, (T_0{}^2)_0)$, λ and a stop criterion , i.e., k or ϵ $\Bigg($iteration number or size of $\left\|(\triangle\kappa_i, \triangle G_i, \triangle(T_0{}^2)_i)\right\|_2\Bigg)$.

Step2. Calculate $\left(\triangle\kappa_i, \triangle G_i, \triangle(T_0{}^2)_i\right)$ using 3.2 and set $\left(\kappa_{i+1}, G_{i+1}, (T_0{}^2)_{i+1}\right) = \left(\kappa_i, G_i, (T_0{}^2)_i\right) + \left(\triangle\kappa_i, \triangle G_i, \triangle(T_0{}^2)_i\right)$

Step3. Stop when the stopping criterion is achieved.

4. Implementation of the method: Examples and results

In this section, we explain the results of the examples and give technical details about the implementation of the algorithm. The examples are simulated by using synthetic noise free data for stiff and soft materials respectively. The optimal values for both examples are preset. The measured output data which is required to solve the inverse problem (in our case $\mathcal{M}(t_i)$'s) is obtained from the numerical solution of the direct problem for the optimal values of $\left(\kappa, G, , {T_0}^2\right)$. The direct problem is solved using the semi-implicit finite difference scheme given in Section2. This scheme involves choosing the size of the meshgrid $N_1 \times N_2$, time step τ and the initial approximation u_0. A brief summary of the error analysis of these variables has been provided in the Section2. In solving the inverse problem, the algorithm requires an initial vector $\kappa_0, G_0, ({T_0}^2)_0$ and a stopping criterion. In each step of the inverse problem algorithm, the solution of each direct problem is found by using the same size of the meshgrid $N_1 \times N_2$, the same time step τ and the same initial approximation u_0 as above. The stop criterion for the iteration is 100 or $\epsilon = 0.01$ $\left(\left\|(\triangle\kappa_i, \triangle G_i, \triangle({T_0}^2)_i\right\|_2 = 0.01\right)$. Whichever is achieved first stops the algorithm. In computing the integral in (3.1), the trapezoid rule is used and the meshgrid $N_1 \times N_2$ is taken as above.

In both examples, the inverse algorithm is first applied to the noise-free synthetic data. Then a 4% noise is added to the initial data (hence $\mathcal{M}(t_i)$ is taken to be 1.04 $\mathcal{M}(t_i)$) and the algorithm is run using the same initial values that have been used for the noise free data. Since the processing time for the algorithm is considerably high for Example 1, we examine the noisy data only in Example 2. The results are obtained and a relative error is calculated for each result corresponding to each initial value. The relative error is used because the numerical values of $u(x, y, t)$ is already small. The relative error is calculated as the following:

$$e = \frac{\left\|u_{\kappa,G,{T_0}^2}(x, y, t) - u_{\kappa',G',{T_0'}^2}(x, y, t)\right\|}{\left\|u_{\kappa,G,{T_0}^2}(x, y, t)\right\|},$$

where $u_{\kappa,G,{T_0}^2}(x, y, t)$ is the solution of the direct problem corresponding to $f_{\kappa,G,{T_0}^2}$ and $\kappa', G', {T_0'}^2$ denote the preset values (hence optimal

values) in each example and the norm is defined as

$$\|u(x,y,t)\| = \max_{t_i}\left(\sum_{k,m} u(x_k,y_m,t_i)^2\right),$$

where $i = 1\cdots q$, $k = 1\cdots N_1$ and $m = 1\cdots N_2$. For each initial guess, the relative error for the noisy data is observed, then the algorithm is run for the noisy data using the initial guess with the biggest relative error with several regularization parameters (in our case since all relative errors are same, we take the first initial guess). Now we examine the algorithm with two inverse problems.

Example 1. In this example $\kappa = 0.5, G = 80.77$ and ${T_0}^2 = 0.027$ are preset for the problem. The algorithm is run for different initial values of $\kappa, G, {T_0}^2$ for the noise-free data. Table 4 shows the initial guesses and the results obtained for the first example. We note that the data in Table 4 is obtained for the meshgrid $N_1 \times N_2 = 41 \times 41$ and (number t_i's) $q = 101$.

Example 2. In this example $\kappa = 0.7, G = 42.33$ and ${T_0}^2 = 0.020$ are preset for the problem. The algorithm is run for different initial values of $\kappa, G, {T_0}^2$ for both noise-free data and noisy data. Table 5 shows the initial guesses and the results obtained for the second example. We note that the data in Table 5 is obtained for the meshgrid $N_1 \times N_2 = 41 \times 41$ and (number t_i's) $q = 31$. Table 6 shows the results for the noisy data. Table 7 shows the results for different choices of regularization parameters and relative error for a chosen initial guess.

Now we give some remarks on the implementation of the algorithm. The main factor affecting the algorithm's efficiency and the precision is the initial guess for κ, G and ${T_0}^2$. In noisy free case, the initial guess has to be made close enough to the optimal values. If the initial guesses are far from the optimal values, either the inverse algorithm fails to converge to a value, mostly due to singularity of $A^{\mathbf{T}}A$ or converges to a value which is not optimal. The latter case is normal because the discrete error functional can have many local minimizers. In this case, if some upper and lower bounds for κ, G and ${T_0}^2$ are already known, one can make a small lattice of initial points within these bounds, then run the algorithm at each lattice point and get results and refine the initial points.

In noisy data case, the ill-posedness of the inverse problem becomes clear. As seen in Table 6, the algorithm converges to a value which is far from the optimal values of κ, G and ${T_0}^2$. However, the relative error in terms of the solution of the direct problem seems to be as small as 0.0029. This is compatible with the theoretical predictions stated in previous sections about inverse problems: one can get same solution for different choices of f. The convergence of the algorithm remains to be a big advantage of the algorithm in noisy data case. In order to fix the results in noisy data case, several choices of regularization parameters are used for the first initial guess. Table 7 clearly shows that the regularization parameters does not change the results and relative errors. Besides the constant regularization parameters given in Table 7, also changing the regularization in each step of the algorithm is applied. The results are not established here because it does not change results as well. To the best of our knowledge, there is no well-established way of choosing regularization parameters for nonlinear inverse problems. One obvious help of the regularization parameter is that it prevents $AA^{\mathbf{T}}$ getting singular which emerges in some cases related to meshgrid sizes of the direct problem.

In the implementations using the optimal mesh grid sizes given in Table 1 for the solution of the direct problem at each step seems to contribute to the precision of the inverse problem algorithm, however it is very costly in processing time. Another key factor in inverse algorithm turns out to be the number of t_i's, i.e., q. In Example 1, taking $q = 11$ or less leads to the singularity of $AA^{\mathbf{T}}$. In that case, one can make use of regularization parameter to run the algorithm but the convergence of the algorithm and the precision of the results will be unsafe. In our experiments, $q = 31$ seems to work well. In Example 1, taking $q = 101$ seems to work well. These observations imply that using the optimal $N_1 \times N_2$ and u_0 in the solution of the direct problem in the inverse problem algorithm works well and the larger the number t_i's, the more stable the results are. However, taking $q = 101$ extends the processing time of the algorithm enormously. If the processing time is not important for an application, our observations have shown that in each problem it is better to use the optimal meshgrid size given in Table 1.

In summary, the main factors affecting the efficiency and the accuracy of the algorithm are the initial guesses and the mesh grid sizes in both problems. In noisy data case the initial guesses turned out to be more important. Using regularization parameter seems to make algorithm converge to some results, however, it is obviously not the

optimal ones. There are also some possible research directions in this problem about the relation of regularization parameter and small mesh grid sizes.

5. Concluding Remarks

We study an inverse problem for the nonlinear evolution equation $u_t - \nabla.\Big(f(T^2)\nabla u\Big) = 2t,\ (x,y,t) \in \Omega_{\mathcal{T}} := \Omega \times (0,\mathcal{T}),\ \Omega \subset \mathbb{R}^2.$ The inverse problem consists of determining the unknown coefficient $f = f(T^2), T^2 := |\nabla u|^2$ by measured output data. The measured output data is nonlocal and has a precise physical meaning: It is the tendency of a force to rotate an object about an axis. In the inverse problem, we determine three unknown parameters of the function $f = f(T^2)$ simultaneously for stiff and soft engineering materials. After we solve the direct problem, we reformulate the inverse problem as a minimization problem. Then a method based on discretization of the minimization problem, steepest descent method and least squares approach is proposed for the numerical solution of the inverse problem. The inverse problem is solved for both noise free and noisy data. The results illustrate applicability and accuracy of the proposed method to some extent.

The authors of this paper plan to consider determination of $f = f(T^2), T^2 := |\nabla u|^2$ from the nonlocal nonlinear equation: $\frac{\partial^\beta}{\partial t^\beta}u(x,y,t) - \nabla.\big(f(T^2)\nabla u\big) = 2t,\ (x,y,t) \in \Omega_{\mathcal{T}}$, where $\beta \in (0,1)$ is the fractional order of the time derivative, $\frac{\partial^\beta}{\partial t^\beta}u(x,t)$ is the Caputo time-fractional derivative of the order $0 < \beta < 1$. This nonlocal equation represents elastoplastic torsion in an environment where anomalous torsion takes place. After establishing existence and/or uniqueness of the solution theoretically, we use the method proposed in this paper to solve the inverse problem.

We also consider to use our method for solving some inverse problems for which the minimization problem can be written in a suitable form to apply least squares approach.

TABLE 4. Results for noise-free for given initial guesses.

Initial Guesses	Results
(0.5,60,0.01)	(0.5,80.8054,0.0269)
(0.3,90,0.03)	(0.5,80.7558,0.0270)
(0.4,95,0.05)	(0.5,80.8016,0.0269)
(0.35,100,0.01)	(0.5,80.7880,0.0270)

TABLE 5. Results for noise-free for different initial guesses.

Initial Guesses	Results
(0.6,35,0.015)	(0.7001,42.3466,0.0196)
(0.8,50,0.025)	(0.7001,42.3437,0.0197)
(0.55,55,0.01)	(0.7001,42.3444,0.0196)
(0.75,60,0.03)	(0.6999,42.2563,0.0204)
(0.78,30,0.015)	(0.7000,42.3138,0.0199)
(0.6,50,0.027)	(0.7001,42.3444,0.0196)

TABLE 6. Results for noisy data for given initial guesses with corresponding relative errors.

Initial Values	Results	Relative Error
(0.6,35,0.015)	(0.7901,113.7292,0.3142)	0.0029
(0.8,50,0.025)	(0.7887,113.7249,0.3189)	0.0029
(0.55,55,0.01)	(0.7880,113.7249,0.3212)	0.0029
(0.75,60,0.03)	(0.7901,113.7291,0.3139)	0.0029
(0.78,30,0.015)	(0.7889,113.7254,0.3181)	0.0029
(0.6,50,0.027)	(0.7902,113.7293,0.3137)	0.0029

6. ACKNOWLEDGMENTS

This research has been supported by the Scientific and Technological Research Council of Turkey (TÜBİTAK) through the project Nr 113F373, also by the Zirve University Research Fund.

TABLE 7. Results for noisy data for a chosen initial guess with different regularization parameters and corresponding relative errors.

Initial Values	Results	Regularization Parameters	Relative Error
(0.6,35,0.015)	(0.7902, 113.8854, 0.3148)	1	0.0029
(0.6,35,0.015)	(0.7901, 113.8854, 0.3149)	2^{-1}	0.0029
(0.6,35,0.015)	(0.7901, 113.8854, 0.3149)	2^{-2}	0.0029
(0.6,35,0.015)	(0.7888, 113.8818, 0.3196)	2^{-3}	0.0029
(0.6,35,0.015)	(0.7901, 113.8855, 0.3149)	2^{-4}	0.0029
(0.6,35,0.015)	(0.7901, 113.8855, 0.3149)	2^{-5}	0.0029
(0.6,35,0.015)	(0.7901, 113.8855, 0.3149)	2^{-6}	0.0029
(0.6,35,0.015)	(0.7892, 113.8829, 0.3181)	10^{-6}	0.0029

REFERENCES

[1] B. Lundberg. Determination of mechanical material properties from the two-point response of an impacted linearly viscoelastic rod specimen. *Journal of Sound and Vibration*, 126:97-108, 1988. 1

[2] L. M . Farrissey and P. E. McHugh Determination of elastic and plastic material properties using indentation: Development of method and application to a thin surface coating. *Materials Science and Engineering A.*, 399:254-266, 2005. 1

[3] A. Hasanov. Simultaneous determination of source terms in a linear parabolic problem from the final overdetermination: Weak solution approach. *Journal of Math. Analys. and Appl.*, 330, 766-779, 2007. 3

[4] A. Hasanov. Simultaneous determination of the source terms in a linear hyperbolic problem from the final overdetermination: weak solution approach. *IMA Journal of Applied Mathematics*, 74, 1-19, 2009. 3

[5] A. Hasanov. Identification of an unknown source term in a vibrating cantilevered beam from final overdetermination. *Inverse Problems*, 25, 115015, 2009. 3

[6] A. Hasanov and S. Tatar. Solutions of linear and nonlinear problems related to torsional rigidity of a beam. *Computational Materials Sciences*, 45, 494-498, 2009. 1, 2, 2

[7] A. Hasanov and S. Tatar. Semi-analytic inversion method for determination elastoplastic properties of power hardening materials from limited torsional experiment. *Inverse Problems in Science and Engineering*, 18, 265-278, 2010. 1, 2, 3

[8] A. Hasanov and S. Tatar. An inversion method for identification of elastoplastic properties of a beam from torsional experiment. *International journal of Nonlinear Mechanics*, 45, 562-571, 2010. 1, 2, 3

[9] C. Heinrich, A. M. Waas, A. S. Wineman. Determination of material properties using nanoindentation and multiple indenter tips. *International Journal of Solids and Structures*, 46, 364-376, 2009. 1

[10] Z. Ismail, H. Khov, and W. L. Li. Determination of material properties of orthotropic plates with general boundary conditions using Inverse method and Fourier series. *Measurement*, 46, 1169-1177, 2013. 1

[11] L. M. Kachanov. Fundamentals of the Theory of Plasticity. *Applied Mathematics and Mechanics 65, North-Holland Publishing Company, Amsterdam-London*, 1971. 1, 1

[12] A. Langenbach. Verallgemeinerte und exakte Losungen des Problems der elastischen-plastischen Torsion von Stabben. *Mathematische Nachrichten* , 28, 219-234, 1971. 1, 1

[13] G. Li, D. Zhang, X. Jia and M. Yamamato. Simultaneous inversion for the space-dependent diffusion coefficient and the fractional order in the time fractional diffusion equation. *Inverse Problems*, 29:065014, 2013. 1

[14] A. Mamedov. An inverse problem related to the determination of elastoplastic properties of a cylindrical bar. *International Journal of Nonl. Mech*, 30:23-32, 1995. 1

[15] T. Nakamura, T. Wang and S. Sampath. Determination of properties of graded materials by inverse analysis and instrumented indentation. *Acta Materialia*, 48, 4293-4306, 2000. 1

[16] M. Moghaddam, W. C. Chew, X. Jia and M. Yamamato. Simultaneous inversion of compressibility and density in the acoustic inverse problem. *Inverse Problems*, 9:715, 1993. 1

[17] Y. H Ou, A. Hasanov, Z. H. Liu. Inverse Coefficient Problems for Nonlinear Parabolic Differential Equations. *Acta Mathematica Sinica, English Series*, 24, 1617-1624, 2008. 3

[18] A. D. Polyanin. Handbook of Linear Partial Differential Equations for Engineers and Scientists. *Chapman & Hall/CRC Press, Boca Raton*, 2002. 2

[19] D. H. Robbins and J. L. Wood. Determination of mechanical properties of the bones of the skull. *Experimental Mechanics*, 9, 236-240, 1960. 1

[20] S. Shen, F. Liu, Q. Liu and V. Anh. Numerical simulation of anomalous infiltration in porous media. *Numer Algor*, DOI: 10.1007/s11075-014-9853-9. 2

[21] A. K. Soh. Determination of the mechanical properties of a composite using the least squares method. *Applied Mathematical Modeling*, 17, 9552-9561, 2013. 1

[22] S. Tatar. Monotonocity of input-output mapping related to inverse elastoplastic torsional problem. *Applied Mathematical Modeling*, 17, 271-278, 1993. 1, 2

[23] S. Tatar. Numerical solution of the nonlinear direct problem related to inverse elastoplastic problem. *Inverse Problems in Science and Engineering*, 21, 52-62, 2013. 1, 2

[24] S. Tatar and Z. Muradoglu. A modification of the semi-analytic inversion method: Determination of the yield stress and a comparision with the parametrization algorithm. *Inverse Problems in Science and Engineering*, 22, 543-556, 2014. 1, 3

[25] S. Tatar and Z. Muradoglu. Numerical solution of the nonlinear evolutional inverse problem related to elatoplastic torsional problem. *Applicable Analysis*, 93, 1187-1200, 2014. 1, 1, 2, 3

[26] S. Tatar, R. Tinaztepe and S. Ulusoy. Simultaneous inversion for the exponents of the fractional time and space derivatives in the space-time fractional diffusion equation. *Applicable Analysis: An International Journal*, DOI: 10.1080/00036811.2014.984291. 1

[27] Q. B. Zhang and J. Zhao. Determination of mechanical properties and full-field strain measurements of rock material under dynamic loads. *International Journal of Rock Mechanics & Mining Sciences*, 93, 1187-1200, 2014. 1

(Salih Tatar)
Department of Mathematics
Faculty of Education
Zirve University
27260, Turkey
E-mail address: salih.tatar@zirve.edu.tr
URL: http://person.zirve.edu.tr/statar/

(Ramazan Tinaztepe)
Department of Mathematics
Faculty of Education
Zirve University
27260, Turkey
E-mail address: ramazan.tinaztepe@zirve.edu.tr
URL: http://person.zirve.edu.tr/tinaztepe/

(Zahir Muradoglu)
Department of Mathematics
Faculty of Art and Sciences
Kocaeli University
41380, Turkey
E-mail address: zahir@kocaeli.edu.tr
URL: http://akademikpersonel.kocaeli.edu.tr/zahir/